Available online at www.sciencedirect.com

ScienceDirect

Mendeleev Commun., 2024, **34**, 650–652

Mendeleev Communications

Symmetry relationships between hybrid lead halide perovskite-derived phases: vacancy ordering as a key classification factor

Ekaterina I. Marchenko,*[a,b] Elena A. Kobeleva,[b] Nikolay N. Eremin,[b,c] Eugene A. Goodilin[a,d] and Alexey B. Tarasov*[a,d]

[a] *Department of Materials Science, M. V. Lomonosov Moscow State University, 119991 Moscow, Russian Federation. E-mail: marchenko-ekaterina@bk.ru, alexey.bor.tarasov@yandex.ru*
[b] *Department of Geology, M. V. Lomonosov Moscow State University, 119991 Moscow, Russian Federation*
[c] *Institute of Geology of Ore Deposits, Petrography, Mineralogy, and Geochemistry, Russian Academy of Sciences, 119017 Moscow, Russian Federation*
[d] *Department of Chemistry, M. V. Lomonosov Moscow State University, 119991 Moscow, Russian Federation*

DOI: 10.1016/j.mencom.2024.09.008

For the first time, based on symmetry group–subgroup relationships, an approach is presented to create a clear classification of hybrid lead halides with low-dimensional vacancy-ordered perovskite-related crystal structures to facilitate the identification and prediction of hybrid lead-halide materials that have desired properties.

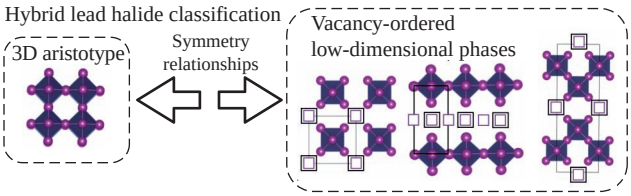

Keywords: hybrid halide perovskites, classification, symmetry relationships, perovskite-related phases, defects, crystal structure.

Hybrid organic–inorganic perovskites of the general formula ABX_3 [A = $MeNH_3^+$, $CH(NH_2)_2^+$; B = Pb^{2+}, Sn^{2+}; X = I^-, Br^-] and their low-dimensional derivatives with different organic cations exhibit a combination of outstanding properties, such as high absorption coefficients, enhanced charge carrier mobility and intense luminescence, and thus represent a new promising class of materials for optoelectronics.[1–4] Some approaches to the rational classification of these compounds with vertex-connected BX_6 octahedra have been proposed in previous works.[5,6] One advantage of hybrid perovskites, as opposed to all-inorganic perovskites, is their ability to accommodate a wide range of defects in a flexible structural framework. Indeed, there are many compounds in which the presence of large cations leads to the formation of partially ordered or disordered vacancies in hybrid halide perovskites. The number and topology of vacancies, along with other crystal chemical characteristics of the structures of hybrid halides (lengths and angles of bonds in BX_6 octahedra,[7] position of the center of mass of the organic cation,[8] *etc.*) affect the optoelectronic properties of these materials.

Generally, all these crystal structures are divided depending on the dimensionality of the inorganic substructure into three-dimensional (3D) perovskite, two-dimensional (2D) hybrid perovskites, as well as one-dimensional (1D) and zero-dimensional (0D) phases.[5] Perovskite-derived hybrid crystal structures include structural motifs of vertex-connected octahedra forming 2D layers and 1D chains. For example, 2D hybrid halide perovskites can be viewed as the result of cutting the 3D parent compound along specific crystallographic planes, as reflected by the general formula $(A')_{2/q}A_{n-1}B_nX_{3n+1}$, where $[A']^{q+}$ is a singly (q = 1) or doubly (q = 2) charged organic spacer cation, A^+ is a small singly charged cation such as Cs^+, $MeNH_3^+$ or $[HC(NH_2)_2]^+$, B^{2+} is Pb^{2+}, Sn^{2+}, *etc.*, X^- is Cl^-, Br^-, I^- and n is the number of layers of corner-shared octahedra within the perovskite slab.[9] There are also varieties of '2.5D' hybrid lead halide perovskite-derived crystal structures (so-called 'hollow' phases),[10,11] in which ordered vacancies of B^{2+} ions and halogens are observed. However, such a classification is not universal, since explicit symmetry relationships between structures are often not indicated. Other approaches to the classification of hybrid halides involve the application of the close-packing theory to compounds of this class, which is also not general, but is applicable only to a limited number of compounds, such as hybrid solvates[12] and hybrid hexagonal close-packed

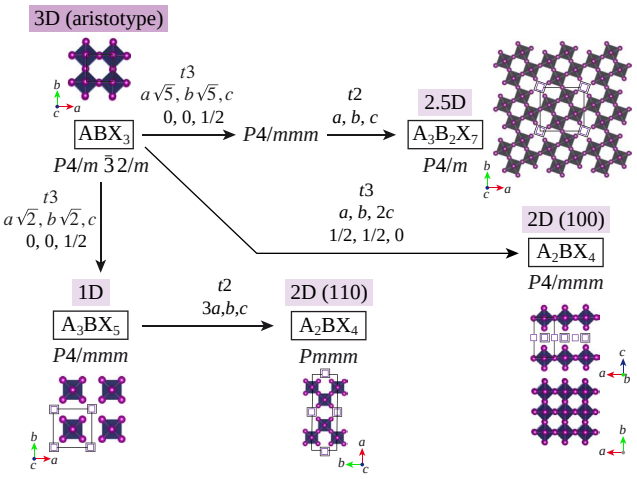

Figure 1 Schematic representation of group–subgroup relationships between 3D aristotype (perovskite) and low-dimensional hettotypes. The nodes consist of Hermann–Mauguin symbols for space group type and formulas. Vacancy sites of inorganic substructure ions are shown by squares. Organic cations have been omitted for clarity. BX_6 octahedra are shown in polyhedral representation. Links are annotated with the kind and index of the relationship, as well as the cell basis transformation (if applicable).

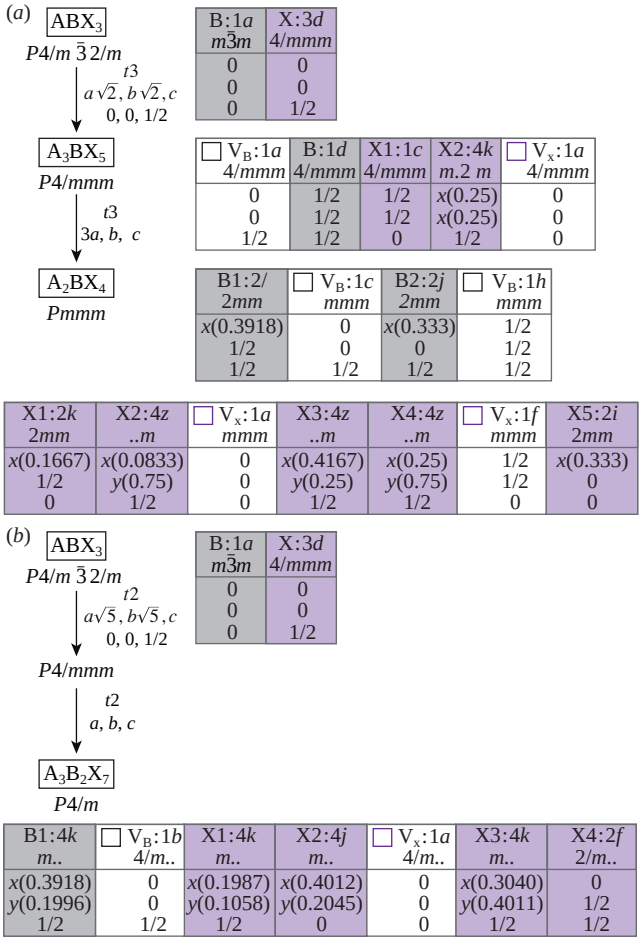

B:1*a* *m*3̄*m*	X:3*d* 4/*mmm*
0	0
0	0
0	1/2

□ V_B:1*a* 4/*mmm*	B:1*d* 4/*mmm*	X1:1*c* 4/*mmm*	X2:4*k* *m*.2 *m*	□ V_x:1*a* 4/*mmm*
0	1/2	1/2	*x*(0.25)	0
0	1/2	1/2	*x*(0.25)	0
1/2	1/2	0	1/2	0

B1:2/ 2*mm*	□ V_B:1*c* *mmm*	B2:2*j* 2*mm*	□ V_B:1*h* *mmm*
x(0.3918)	0	*x*(0.333)	1/2
1/2	0	0	1/2
1/2	1/2	1/2	1/2

X1:2*k* 2*mm*	X2:4*z* ..*m*	□ V_x:1*a* *mmm*	X3:4*z* ..*m*	X4:4*z* ..*m*	□ V_x:1*f* *mmm*	X5:2*i* 2*mm*
x(0.1667)	*x*(0.0833)	0	*x*(0.4167)	*x*(0.25)	1/2	*x*(0.333)
1/2	*y*(0.75)	0	*y*(0.25)	*y*(0.75)	1/2	0
0	1/2	0	1/2	1/2	0	0

B:1*a* *m*3̄*m*	X:3*d* 4/*mmm*
0	0
0	0
0	1/2

B1:4*k* *m*..	□ V_B:1*b* 4/*m*..	X1:4*k* *m*..	X2:4*j* *m*..	□ V_x:1*a* 4/*m*..	X3:4*k* *m*..	X4:2*f* 2/*m*..
x(0.3918)	0	*x*(0.1987)	*x*(0.4012)	0	*x*(0.3040)	0
y(0.1996)	0	*y*(0.1058)	*y*(0.2045)	0	*y*(0.4011)	1/2
1/2	1/2	1/2	0	0	1/2	1/2

Figure 2 Symmetry relationships between crystal structures derived from perovskite with ordered vacancies as the inorganic substructural motif transitions (*a*) from 3D to 1D and 2D (110), and (*b*) from 3D to 2.5D. The nodes consist of Hermann–Mauguin symbols for space group type, compound formulas and occupied/unoccupied Wyckoff positions of inorganic substructures. Links are annotated with the kind and index of the relationship, as well as the cell basis transformation (if applicable).

polytypes.[13] Symmetry group–subgroup relationships have been used to describe the incommensurately modulated phases of 3D hybrid halide perovskites.[14] In this work, we developed an advanced classification of hybrid lead halides with low-dimensional vacancy-ordered inorganic substructures related to perovskites using symmetry group–subgroup relationships and the Bärnighausen formalism.[15,16]

We constructed an idealized Bärnighausen tree (Figure 1) showing group–subgroup relationships between the 3D hybrid halide, called aristotype (*G*), and the 1D, 2D and 2.5D derivatives with ordered vacancies in the inorganic substructure, called hettotypes (*H*). The most symmetrical cubic 3D structure ABX_3, which belongs to the perovskite structure type with space group $Pm\bar{3}m$, does not contain vacancies in the inorganic substructure. Low-symmetry derivatives of this structure, *i.e.*, hettotypes, are vacancy-ordered phases: 1D A_3BX_5 (space group *P*4/*mmm*), 2D (110) A_2BX_4 (space group *Pmmm*), 2D (100) A_2BX_4 (space group *P*4/*mmm*) and 2.5D $A_3B_2X_7$ (space group *P*4/*m*). The scheme shows idealized models of crystal structures with higher symmetry groups without distortions of the metal halide octahedra and

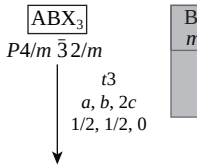

B:1*a* *m*3̄*m*	X:3*d* 4/*mmm*
0	0
0	0
0	1/2

B1:1*c* 4/*mmm*	□ V_B:1*d* 4/*mmm*	X1:2*f* *mmm*.	X2:2*h* 4*mm*	□ V_x:2*e* *mmm*
1/2	1/2	0	1/2	0
1/2	1/2	1/2	1/2	1/2
0	1/2	0	*z*(0.75)	1/2

Figure 3 Symmetry relationships between 3D and vacancy-ordered 2D (100) crystal structures. The nodes consist of Hermann–Mauguin symbols for space group type, compound formulas and occupied/unoccupied Wyckoff positions of inorganic substructures. Links are annotated with the kind and index of the relationship, as well as the cell basis transformation.

rotations of the octahedra relative to each other. Organic cations have been omitted for clarity. The group–subgroup transition from the aristotype to the 1D structure with chains of vertex-connected octahedra in the inorganic substructure is represented by a *t*-type transition† with a symmetry reduction index of 3 and a change in the unit cell parameters as $a\sqrt{2}$, $b\sqrt{2}$, c and a shift of the unit cell origin along the vector (0, 0, 1/2). This structure contains chains of metal and halogen vacancies alternating with chains of BX_6 octahedra, as shown in Figure 1.

Other group–subgroup transitions were described in a similar manner. All group–subgroup relationships are accompanied by a decrease in the symmetry group, a change in the cell parameters relative to the aristotype and the presence of ordered vacancies in the inorganic substructure. To comply with the rule, the transition from a 3D structure to a 2.5D structure (space group *P*4/*m*) must pass through the intermediate tetragonal group *P*4/*mmm*.[1]

In addition to describing group–subgroup relationships and changes in unit cell parameters, our classification contains strict correspondences in terms of the splitting of crystallographic sites between aristotype and hettotype structures (Figures 2 and 3). The symmetry of the sites of ions and vacancies in structures is reflected in the form of Wyckoff positions[17] and their coordinates. The positions of vacancies, B ions and X anions are shown in white, gray and violet, respectively. As symmetry in structures decreases, the number of different crystallographic sites for ions and vacancies increases.

In summary, our approach shows that it is possible to introduce a systematic order of hybrid halide perovskite-related phases using symmetry relationships as a guiding principle. We believe that the constructed group–subgroup relationships provide a convenient classification of hybrid halide perovskite-related compounds and could probably be leveraged as a useful tool for developing machine learning algorithms to classify structures and identify correlations between composition, structure and properties of materials.

This work was supported by the Russian Science Foundation (grant no. 23-73-01212, https://rscf.ru/project/23-73-01212/).

References

1 W. Li, Z. Wang, F. Deschler, S. Gao, R. H. Friend and A. K. Cheetham, *Nat. Rev. Mater.*, 2017, **2**, 16099; https://doi.org/10.1038/natrevmats.2016.99.
2 J. Huang, Y. Yuan, Y. Shao and Y. Yan, *Nat. Rev. Mater.*, 2017, **2**, 17042; https://doi.org/10.1038/natrevmats.2017.42.
3 N.-G. Park, M. Grätzel, T. Miyasaka, K. Zhu and K. Emery, *Nat. Energy*, 2016, **1**, 16152; https://doi.org/10.1038/nenergy.2016.152.
4 J.-C. Blancon, J. Even, C. C. Stoumpos, M. G. Kanatzidis and A. D. Mohite, *Nat. Nanotechnol.*, 2020, **15**, 969; https://doi.org/10.1038/s41565-020-00811-1.
5 B. Saparov and D. B. Mitzi, *Chem. Rev.*, 2016, **116**, 4558; https://doi.org/10.1021/acs.chemrev.5b00715.

† For this kind of procedure, C. Hermann's theorem is of particular importance. There are some special kinds of subgroups (*H*) of a space group (*G*). *G* is a space group with point group P_G. *H* is a normal subgroup of all translations T_G. $H < G$ is called a *translationengleiche* (*t*) subgroup if *G* and *H* have the same group of translations; therefore, *H* belongs to a crystal class of lower symmetry than *G*, $P_H < P_G$.

6 J. A. McNulty and P. Lightfoot, *IUCrJ*, 2021, **8**, 485; https://doi.org/10.1107/S2052252521005418.
7 E. I. Marchenko, V. V. Korolev, S. A. Fateev, A. Mitrofanov, N. N. Eremin, E. A. Goodilin and A. B. Tarasov, *Chem. Mater.*, 2021, **33**, 7518; https://doi.org/10.1021/acs.chemmater.1c02467.
8 E. I. Marchenko, S. A. Fateev, A. A. Ordinartsev, P. A. Ivlev, E. A. Goodilin and A. B. Tarasov, *Mendeleev Commun.*, 2022, **32**, 315; https://doi.org/10.1016/j.mencom.2022.05.007.
9 E. I. Marchenko, S. A. Fateev, A. A. Petrov, V. V. Korolev, A. Mitrofanov, A. V. Petrov, E. A. Goodilin and A. B. Tarasov, *Chem. Mater.*, 2020, **32**, 7383; https://doi.org/10.1021/acs.chemmater.0c02290.
10 T. Ohmi, I. W. H. Oswald, J. R. Neilson, N. Roth, S. Nishioka, K. Maeda, K. Fujii, M. Yashima, M. Azuma and T. Yamamoto, *J. Am. Chem. Soc.*, 2023, **145**, 19759; https://doi.org/10.1021/jacs.3c05390.
11 J. A. McNulty, A. M. Z. Slawin and P. Lightfoot, *Dalton Trans.*, 2020, **49**, 15171; https://doi.org/10.1039/D0DT03449E.
12 A. A. Petrov, E. I. Marchenko, S. A. Fateev, Y. Li, E. A. Goodilin and A. B. Tarasov, *Mendeleev Commun.*, 2022, **32**, 311; https://doi.org/10.1016/j.mencom.2022.05.006.
13 E. I. Marchenko, S. A. Fateev, V. V. Korolev, V. Buchinskiy, N. N. Eremin, E. A. Goodilin and A. B. Tarasov, *J. Mater. Chem. C*, 2022, **10**, 16838; https://doi.org/10.1039/D2TC03202C.
14 D. Wiedemann, J. Breternitz, D. W. Paley and S. Schorr, *J. Phys. Chem. Lett.*, 2021, **12**, 2358; https://doi.org/10.1021/acs.jpclett.0c03722.
15 H. Bärnighausen, *MATCH*, 1980, **9**, 139; https://match.pmf.kg.ac.rs/electronic_versions/Match09/match9_139-175.pdf.
16 U. Müller, *Symmetry Relationships between Crystal Structures: Applications of Crystallographic Group Theory in Crystal Chemistry*, Oxford University Press, Oxford, 2013; https://global.oup.com/academic/product/symmetry-relationships-between-crystal-structures-9780199669950.
17 R. W. G. Wyckoff, *The Analytical Expression of the Results of the Theory of Space-Groups*, Carnegie Institution of Washington, Washington, 1922; https://books.google.com/books/about/The_Analytical_Expression_of_the_Results.html?id=HTRUAAAAMAAJ.

Received: 13th May 2024; Com. 24/7496